

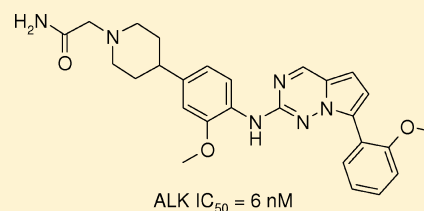
Strategies to Mitigate the Bioactivation of 2-Anilino-7-Aryl-Pyrrolo[2,1-*f*][1,2,4]triazines: Identification of Orally Bioavailable, Efficacious ALK Inhibitors

Eugen F. Mesaros,* Tho V. Thieu, Gregory J. Wells, Craig A. Zifcsak, Jason C. Wagner, Henry J. Breslin, Rabindranath Tripathy, James L. Diebold, Robert J. McHugh, Ashley T. Wohler, Matthew R. Quail, Weihua Wan, Lihui Lu, Zeqi Huang, Mark S. Albom, Thelma S. Angeles, Kevin J. Wells-Knecht, Lisa D. Aimone, Mangeng Cheng, Mark A. Ator, Gregory R. Ott, and Bruce D. Dorsey

Worldwide Discovery Research, Cephalon, Inc., 145 Brandywine Parkway, West Chester, Pennsylvania 19380, United States

Supporting Information

ABSTRACT: Chemical strategies to mitigate cytochrome P450-mediated bioactivation of novel 2,7-disubstituted pyrrolo[2,1-*f*][1,2,4]triazine ALK inhibitors are described along with synthesis and biological activity. Piperidine-derived analogues showing minimal microsomal reactive metabolite formation were discovered. Potent, selective, and metabolically stable ALK inhibitors from this class were identified, and an orally bioavailable compound (32) with antitumor efficacy in ALK-driven xenografts in mouse models was extensively characterized.



INTRODUCTION

A set of chimeric oncoproteins that contain the catalytic subunit of anaplastic lymphoma kinase (ALK)¹ have been identified in a number of clearly defined cancers,² including anaplastic large cell lymphoma³ (NPM-ALK), non-small cell lung cancer⁴ (EML4-ALK), and inflammatory myofibroblastic tumors⁵ (TPM3-ALK). Aberrant expression of full-length ALK has been implicated in glioblastoma.^{6a} Furthermore, somatic and germline mutations of ALK have been shown to have a causative role in neuroblastoma.^{6b} ALK is a member of the insulin receptor (IR) tyrosine kinase family, and full-length ALK expression is restricted to the central and peripheral nervous systems. The function of ALK has not been completely delineated, although it is believed to be important in the physiological development and function of the nervous system.^{2b} On the basis of disease pathologies associated with dysregulated ALK catalytic activity, a number of ATP-competitive kinase inhibitors have been reported as potential therapies that act by disrupting the signal transduction cascade of constitutively active ALK.⁷ The structures of clinical level inhibitors PF-2341066 (1)^{8a-d} and CH5424802 (2)^{8e} have been published (Figure 1).

Our group has reported ALK inhibitors from diverse structural classes including indolocarbazoles,⁹ tetrahydropyrido-[2,3-*b*]pyrazines,¹⁰ uniquely substituted 2,4-diaminopyrimidines¹¹ (3, Figure 1), and most recently, 2-anilino-7-aryl-pyrrolo[2,1-*f*][1,2,4]triazines (4, Figure 1).¹² Though orally efficacious in ALK-dependent tumor xenografts in mouse, preclinical testing of 4 and related analogues in bioactivation/glutathione (GSH) trapping experiments in liver microsomes identified extensive NADPH-mediated oxidation of the *p*-dianiline moiety to a reactive quinone diimine.¹³ Reactive metabolites of certain drugs have been linked to idiosyncratic adverse drug reactions due to their ability to covalently conjugate endogenous

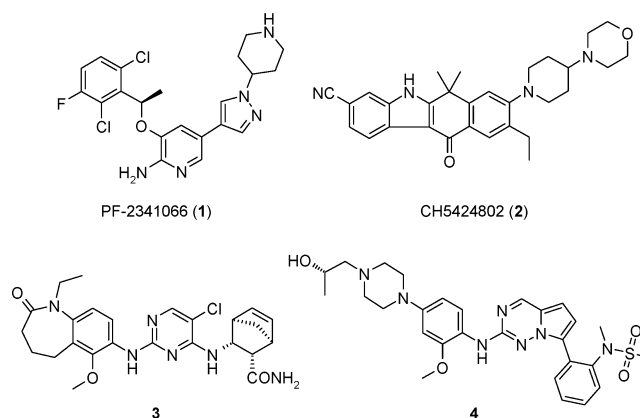


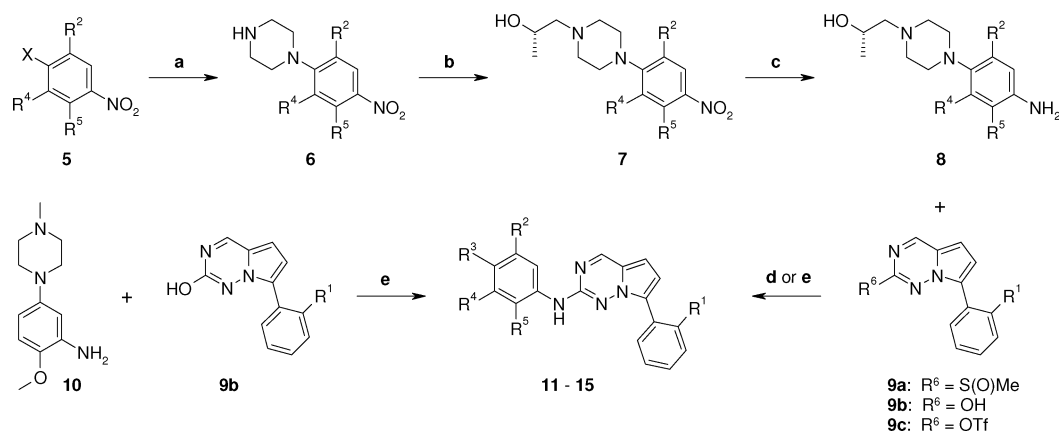
Figure 1. Recently published ALK inhibitors.

macromolecules. Even though generalizations that associate reactive metabolites with toxicities cannot be unequivocally made, bioactivation is perceived as a potential risk.¹⁴ In this context, the remarkable magnitude of bioactivation in this subset of pyrrolo-triazines was quite unexpected by comparison to the much lower levels listed in literature for inhibitors with similar structural motifs.^{13,14} Nevertheless, the postulated mechanism for bioactivation suggested that further structural modifications to the susceptible fragment may attenuate this phenomenon.¹⁴

Herein, we describe a three-pronged strategy to mitigate bioactivation/glutathione addition, including the installation of electron withdrawing substituents to the site of oxidation, shifting the position of the saturated heterocycle on the aniline

Received: August 10, 2011

Published: December 5, 2011

Scheme 1. Synthesis of Piperazine Derivatives 11–15^a

^aReagents and conditions (for R^{1–5} definitions, see Table 1): (a) (i) for X = F (inhibitors 11 and 13), *N*-Boc-piperazine, K₂CO₃, DMF, 60 °C, 60–90%, for X = Br (inhibitor 12), *N*-Boc-piperazine, Pd₂(dba)₃, XantPhos, Cs₂CO₃, 1,4-dioxane, 100 °C, 66%; (ii) TFA, DCM, rt, 80–97%; (b) (*S*)-2-methyl-oxirane, MeOH, 42–82%; (c) H₂, Pd/C, MeOH, 87–97%; (d) 9a (R¹ = N(Me)SO₂Me), DIPEA, 1-methoxy-2-propanol, microwave, 200 °C, 8%; (e) (i) 9b, (F₃CSO₂)₂NPh, DIPEA, DMF, 0 °C → rt; (ii) 8 or 10, 85 °C, 30–47%.

Table 1. Enzyme and Cellular ALK Inhibition Data with Percent Glutathione Adduct for Compounds 4 and 11–15

compd	R ¹	R ²	R ³	R ⁴	R ⁵	IC ₅₀ (nM) ^a		% GSH adducts ^b
						ALK enzyme	ALK cell	
4	–N(Me)SO ₂ Me	H	A	H	–OMe	10 ± 2	60	61
11	–N(Me)SO ₂ Me	H	A	F	–OMe	56 ± 16		12
12	–N(Me)SO ₂ Me	F	A	H	–OMe	14 ± 3	200	13
13	–N(Me)SO ₂ Me	F	A	H	F	91 ± 19		0.8
14	–N(Me)SO ₂ Me	B	H	H	–OMe	28 ± 8		3.9 ^c
15	–OMe	B	H	H	–OMe	187 ± 64		2.3 ^c

^aIC₅₀ values are reported as the average of at least two separate determinations; standard deviations are indicated where at least three determinations were made. ^bRelative to the tested compound. See also ref 13. ^cDue to O-demethylation and iminoquinone formation/trapping.

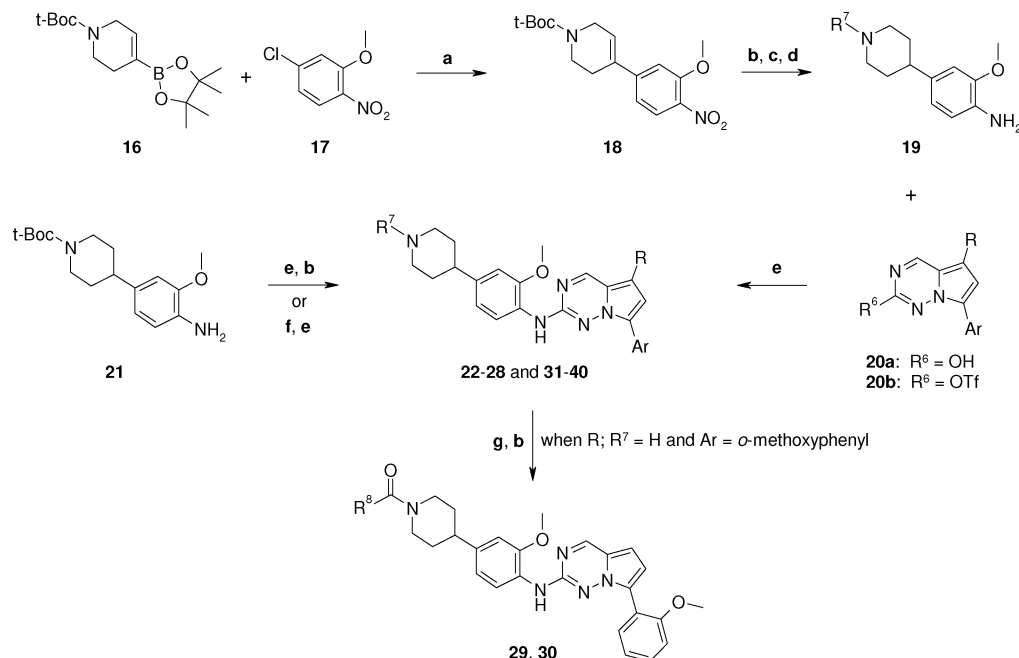
ring, as well as modifying the heterocycle to remove the *p*-nitrogen of the ring. These approaches have led to the identification of an inhibitor that is basically devoid of the bioactivation phenomenon and is also potent in enzymatic and cellular assays, orally bioavailable, and displays antitumor activity in ALK-driven subcutaneous tumor xenografts in mice.

CHEMISTRY

We prepared the novel compounds discussed herein according to synthetic procedures adapted from our previously reported work.^{12,15} The synthesis of inhibitors 11–15 is outlined in Scheme 1 (cf. also Table 1). Commercially available aromatic halides 5 were reacted with *N*-Boc-piperazine, followed by deprotection to generate amines 6, which were next alkylated with (*S*)-2-methyl-oxirane. Nitro groups in 7 were reduced to give anilines 8. Inhibitor 11 was prepared by reacting sulfoxide 9a (R¹ = N(Me)SO₂Me)¹² with the appropriate aniline 8. Superior yields were obtained for compounds 12–15 via 2-step one-pot transformations: conversion of pyrrolotriazin-2-ols 9b¹² to the corresponding trifluoromethanesulfonates 9c, followed by in situ aromatic nucleophilic displacements with anilines 8 or 10.

Inhibitors 22–40 (cf. also Tables 2–4) were prepared according to the general sequence depicted in Scheme 2. Suzuki coupling of commercially available boronic ester 16 and chloride 17 afforded 1,2,3,6-tetrahydropyridine derivative 18. Nitrogen deprotection with trifluoroacetic acid, followed by alkylation of the resulting amine, provided the corresponding nitrophenyl-1,2,3,6-tetrahydropyridine intermediates.

Concurrent catalytic hydrogenation of the olefin and the nitro group afforded precursors 19. Final union of anilines 19 and pyrrolotriazin-2-ols 20a^{12,15} under the same reaction conditions as described earlier generated inhibitors 22, 23, 25, 27, 28, and 31–40. Aniline 21 was obtained by catalytic hydrogenation of 18 and was reacted with pyrrolotriazin-2-ols 9b (with both R¹ = N(Me)SO₂Me and R¹ = OMe). Deprotection of the amine afforded inhibitors such as N–H piperidine 24 (Table 2). Amide coupling reactions followed by Boc-amine deprotection secured amino acid derivatives 29 and 30. Reduction of Boc-amine 21 with LiAlH₄ gave the corresponding *N*-methyl piperidine intermediate which was converted to inhibitor 26 (Table 3).

Scheme 2. Synthesis of Piperidine Derivatives 22–40^a

^aReagents and conditions (for R and R^{1,7,8} definitions, see Tables 2–4): (a) Pd(PPh₃)₄, KHCO₃, water/1,4-dioxane, 80 °C, 97%; (b) TFA, DCM, rt, 95%; (c) for inhibitors 22, 23, 25, 27, 28, epoxide, MeOH, 42–80%; for inhibitors 31–40, BrCH₂CONHMe or ICH₂CONH₂, Cs₂CO₃, MeCN, 75 °C, 71–80%; (d) H₂, Pd/C, MeOH, > 90%; (e) (i) 20a, (F₃CSO₂)₂NPh, DIPEA, DMF, 0 °C → rt; (ii) aniline (e.g., 19 or 21), 85 °C, 13–58%; (f) LiAlH₄, THF, reflux, 92%; (g) *N*-Boc-aminoacid, EDCI, HOBT, DIPEA, DMF 50–60%.

Table 2. Enzyme and Cellular ALK Inhibition Data with Half-Lives (*t*_{1/2}) in Liver Microsomes for Compounds 22–25

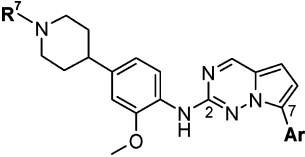
compd	R ¹	R ⁷	IC ₅₀ (nM) ^a		Liver microsome <i>t</i> _{1/2} (min) ^b			
			ALK Enzyme	ALK Cell	M	R	Mo	H
22	-N(Me)SO ₂ Me		6 ± 1	60	> 40	21	< 5	< 5
23	-N(Me)SO ₂ Me		6 ± 2	70	> 40	11	< 5	< 5
24	-N(Me)SO ₂ Me	H	10 ± 4	40	> 40	22	< 5	7
25	-OMe		3.4 ± 0.9	100	> 40	> 40	21	> 40

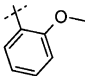
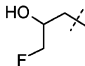
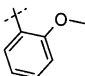
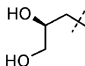
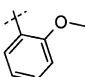
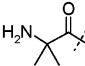
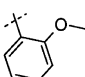
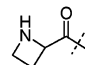
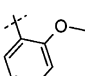
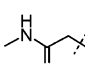
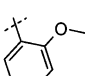
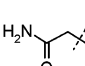
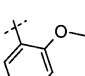
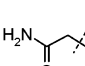
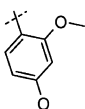
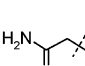
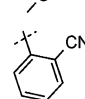
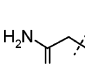
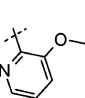
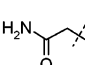
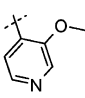
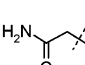
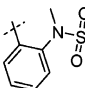
^aIC₅₀ values are reported as the average of at least two separate determinations; standard deviations are indicated where at least three determinations were made. ^bM = mouse; R = rat; Mo = monkey; H = human.

RESULTS AND DISCUSSION

The level of covalent glutathione adduct formed by a xenobiotic that has been incubated with liver microsomes and GSH in the presence of NADPH was deemed a reasonable stratification tool to assess the risk associated with reactive metabolite-related idiosyncratic toxicity.¹³ We set our goal to synthesize analogues with minimal/no in vitro GSH conjugation (reported as % GSH-adduct relative to the tested compound), consistent with literature reports on bioactivation of marketed drugs.^{13,14}

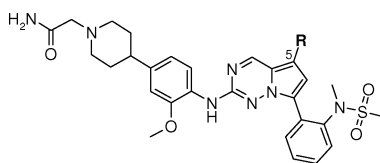
One documented strategy for decreasing metabolic oxidation of aromatics is to lower their electron density.¹⁶ Toward this end, small electron withdrawing groups were installed on the C2-aniline ring (Table 1) to arrive at analogues 11–13. Indeed, monofluorinated derivatives 11 and 12 showed an 80% reduction in adduct formation compared to 4, although the levels of GSH conjugation were still above the threshold considered high risk.¹³ Fluorination was also accompanied by some erosion of activity in ALK enzyme and cell-based primary assays. Enzyme activity of 12 was acceptable (IC₅₀ = 14 nM),

Table 3. Enzyme and Cellular ALK Inhibition Data with IR Inhibition, Kinome Selectivity, and iv Half-Life ($t_{1/2}$), Clearance (CL), and Oral Bioavailability ($F\%$) in Rat for Compounds 26–37


compd	R ⁷	Ar	IC ₅₀ (nM) ^a			S(90) ^b	Rat PK iv data ^c		
			ALK Enzyme	ALK Cell	IR Enzyme		t _{1/2} (h)	CL (mL/min/kg)	Rat F%
26	Me-		6 ± 2	70	222 ± 84	0.10	1.4	29	3
27			3 ± 1	80	149 ± 55	0.09	1.4	62	16
28			2.9 ± 0.9	30	164 ± 42	0.06	2	39	15
29			7 ± 2	150	579 ± 194	0.09	2.6	25	13
30			11 ± 5	200	335 ± 87	-	2.5	32	15
31			10 ± 4	100	161 ± 47	0.04	-	-	-
32			6 ± 2	100	222 ± 81	0.03	3.4	12	43
33			12 ± 4	500	2967 ± 184	-	-	-	-
34			19 ± 6	250	747 ± 274	-	-	-	-
35			1061 ± 460	-	>10000	-	-	-	-
36			9 ± 4	150	410 ± 141	0.06	-	-	-
37			15 ± 4	80	552 ± 62	0.13	-	-	-

^aIC₅₀ values are reported as the average of at least two separate determinations; standard deviations are indicated where at least three determinations were made. ^bKinase selectivity was determined using the Ambit Bioscience KINOMEScan technology, and is expressed as S(90), the fraction of kinases inhibited >90% when screened at 1 μM across a panel of 256 kinases. See ref 19. ^cFor the complete list of PK parameters in rat, see the Supporting Information.

Table 4. Enzyme and Cellular ALK Inhibition Data with Half-Lives in Liver Microsomes and Oral Bioavailability in Rat for Compounds 37–40



compd	R	IC ₅₀ (nM) ^a		liver microsome t _{1/2} (min) ^b				rat F % ^c
		ALK enzyme	ALK cell	M	R	Mo	H	
37	H	15 ± 4	80	29	<5	<5	<5	
38	OH	11 ± 1		<5	<5	<5	<5	
39	Me	6 ± 2	70	>40	31	6	18	24
40	Cl	4.7 ± 0.7	70	>40	>40	15	37	41

^aIC₅₀ values are reported as the average of at least two separate determinations; standard deviations are indicated where at least three determinations were made. ^bM = mouse; R = rat; Mo = monkey; H = human. ^cFor the complete list of PK parameters in rat, see the Supporting Information.

whereas the inhibitory activity against phosphorylation of NPM-ALK in the cell-based assay was modest (IC₅₀ = 200 nM). Difluorinated compound **13** was sufficiently electron-deficient to be resistant to metabolic activation, however, replacing the electron-donating *o*-methoxy group with a fluorine atom contributed to further weakening of ALK inhibition.

Alternatively, shifting the piperazine from the *para*- to *meta*-position of the aniline ring (with respect to C2-NH, cf. Table 1) would negate *p*-diiminoquinone formation, although it would open the possibility of CYP-mediated hydroxylation at the (now) unsubstituted *p*-position (R³ = H) and the potential to form a *p*-iminoquinone. Interestingly, CYP-mediated formation of an iminoquinone was observed, albeit mass spectrometric analysis of the GSH-adduct demonstrated that the product originated from demethylation of the *o*-methoxy unit (R⁵) rather than hydroxylation *para* to C2-NH. The levels of covalent adducts were greatly minimized for **14** and **15** (Table 1) relative to the *p*-piperazine congeners; however, the potency of these analogues was outside of the desired range. Combined with previous structure–activity relationships (SAR),^{11,12} the above studies suggested that the saturated *para*-heterocycle and *ortho*-methoxy group substitutions were critical drivers of potency. This led us to consider an alternative approach to mitigate bioactivation to the *p*-diiminoquinones, namely replacing the piperazine with a piperidine (cf. Table 2). In theory, *p*-CH-anilines would still be capable of bioactivation to quinonemethide imine species; however, the oxidation potential relative to dianilines was expected to be dramatically diminished.

Derivative **22** validated this strategy, generating only 0.2% GSH adduct, via demethylation and bioactivation to the *o*-iminoquinone species with no formation of imino-quinonemethide detected. This very low level of covalent adduct was considered acceptable to pursue this strategy further. Piperidines **22** and **23** (Table 2) were equally active in ALK enzyme and cell assays to piperazine **4**. Interestingly though, they displayed suboptimal stability in liver microsomes.¹⁷ This was unanticipated based on our previous experience with **4** and *ent*-**4**,¹² compounds with liver microsome t_{1/2} > 40 min across all tested species (mouse, rat, monkey, and human). Furthermore, N–H piperidine **24** also displayed poor microsome stability, suggesting that *N*-dealkylation at the piperidine ring was not the major metabolic pathway.

On the basis of the knowledge accumulated with diamino-pyrimidines^{11b} and pyrrolotriazines,¹² we replaced the *o*-*N*-methyl(methylsulfonamide) group on C7-phenyl with *o*-methoxy

to generate analogue **25**. This modification maintained enzyme and cellular ALK activity and, interestingly, restored liver microsome stability. However, the improved stability in rat liver microsomes (t_{1/2} > 40 min; Table 2) did not correlate with the iv parameters from the pharmacokinetic studies: short half-life (t_{1/2} = 0.4 h) and moderately fast clearance (CL = 38 mL/min/kg). Similar stability profile was observed for **25** in the rat S9 fraction in vitro assay (t_{1/2} > 40 min), suggesting that other and possibly nonhepatic clearance mechanisms might play a role in vivo. Exposure after oral dosing in rat was also low (e.g., F < 1%; AUC_{0–∞} = 11 ng·h/mL, with a 5 mg/kg single oral dose; see also the Supporting Information).

Focus turned next to addressing pharmacokinetic properties in rat by diversifying the piperidine N-substitution on analogues with an *o*-methoxyphenyl group at C7 (cf. compounds **26**–**32** in Table 3). *N*-Methylpiperidine **26** was active in cells and showed moderate selectivity against the insulin receptor (IR/ALK IC₅₀ ratio of 37)¹⁸ but at the expense of very low oral exposure in rat. Kinome selectivity,¹⁹ expressed as the fraction of kinases inhibited >90% when screened at 1 μM across a panel of 256 kinases, S(90), was acceptable (≤0.10). Related 2-hydroxypropyl derivatives **27** and **28** showed good ALK activity and acceptable kinase selectivity, including against IR. Of note, diol **28** provided a 3-fold boost in cellular activity; GSH adduct levels in microsomes were 0.5% and oral bioavailability in rat improved to 15%. Amides **29** and **30** showed some erosion in cellular activity but maintained comparable selectivity and oral bioavailability. Notably, the iv half-lives in rat were progressively longer going from compound **26** to **30** (Table 3) and were in good correlation with the in vitro stability in both rat liver microsomes and S9 fraction (t_{1/2} > 40 min for compounds **27**–**30**). With the exception of **27**, the clearance was below the hepatic blood flow (50 mL/min/kg¹²). 2-(*N*-Piperidine)-acetamide derivatives **31** and **32** were equipotent in the ALK cellular assay. Compound **32** was significantly more stable in liver microsomes (t_{1/2} > 40 min in all four species) than **31** (t_{1/2} < 12 min in monkey and human), suggesting that the unsubstituted amide nitrogen is metabolically more favorable. Acetamide **32** had very good ALK activity and kinase selectivity (including against IR). The inhibitory activity against NPM-ALK phosphorylation in cells was also favorable (IC₅₀ = 100 nM). In rat PK experiments, **32** showed a substantial boost in iv half-life (3.4 h) and low clearance (12 mL/min/kg; only 24% of the hepatic blood flow), in excellent correlation with the stability in rat liver microsomes (>40 min). The oral bioavailability (Table 3) was also markedly improved. The propensity

of **32** for bioactivation was minimal (0.6% GSH adduct, from O-demethylation). On the basis of the favorable profile, **32** advanced to in vivo studies (vide infra).

Further SAR exploration of C7-aryl moieties with the optimized acetamide piperidine was undertaken (cf. compounds **33–37** in Table 3). *Para* substitution on the C7 phenyl brought to inhibitor **33** a tremendous increase in IR selectivity, paralleling the corresponding selectivity determinant identified previously in the diaminopyrimidine class.^{11b} However, this improvement came at the cost of lower cell activity. Replacement of *o*-methoxy group in **32** with a nitrile generated analogue **34**, which was 3-fold less active. Regioisomeric 3-methoxy-pyridines **35** and **36** showed dramatically different ALK inhibitory activities.

We postulate that the >100-fold lower activity of **35** (relative to **36**) may be due to electron lone pair repulsions between the pyridyl and the core (N1) nitrogen atoms rendering the dihedral about the C7-aryl bond much larger than required in the active conformation.¹² Similar to **22–24** (Table 2), sulfonamide **37** was active, but metabolically unstable: $t_{1/2} < 5$ min in rat, monkey, and human liver microsomes. Both **36** and **37** showed acceptable levels of IR and kinome selectivity.

At this stage, we decided to reinvestigate *N*-methyl-(methylsulfonamide) derivatives, focusing on the metabolic fate of compound **37** in liver microsomes and anticipating that we would be able to uncover the metabolic “hot-spot.” LC/MS-based metabolite analyses were conducted for **37**, indicating oxidation to a compound of molecular weight ($M + 16$) to be the major pathway in vitro. The fragmentation pattern in the MS/MS spectrum narrowed the possible hydroxylation sites to the pyrrolotriazine core, although the exact position could not be unequivocally established. Suspecting that pyrrole oxidation may have occurred, we prepared C5-hydroxy derivative **38** (Table 4), which showed identical LC retention time and MS/MS spectrum to the ($M + 16$) metabolite of **37**. Thus, blocking the C5 position with either methyl (**39**) or chlorine (**40**) gave substantially more stable analogues (Table 4). Analogues **39** and **40** displayed not only acceptable activity and selectivity profiles (e.g., IR/ALK > 88 for both) but also high oral bioavailability and plasma exposure levels in rat. Similar to **32**, in vitro metabolic stability of **39** and **40** correlated well with the iv half-lives ($t_{1/2} \geq 2$ h) and clearance ($CL \leq 4$ mL/min/kg) in rat. Less than 1% GSH conjugation was observed for **39** and **40** in liver microsomes, again through a *O*-demethylation/oxidation route.

On the basis of the favorable in vitro profiles and pharmacokinetic properties in rat (Tables 3 and 4), **32**, **39**, and **40** were selected for in vivo PK/PD evaluation in tumor xenograft models. Initially, single dose PK/PD studies monitoring ALK signaling in Sup-M2 tumor xenografts in Scid mice along with drug exposure in plasma/tumors were used to assess in vivo activity. Oral dosing of **39** or **40** at 30 mg/kg, po exerted much less than 75% inhibition of NPM-ALK phosphorylation over 12 h, demonstrating that significantly higher doses would be required to achieve sustained target inhibition (see Supporting Information).

Inhibitor **32**, on the other hand, displayed strong inhibition at 30 mg/kg, po (vide infra), which warranted further in vitro and in vivo profiling. In cytotoxicity assays in cell cultures, compound **32** demonstrated concentration-related growth inhibition of ALK-dependent cell lines Sup-M2 and Karpas-299, whereas it had a minimal effect on the viability of ALK-independent cell lines K562 and Hut-102 (see Supporting Information). Upon treatment with **32**, pro-apoptotic caspases

3 and **7** were activated in ALK-dependent cell lines while remaining at basal levels in the ALK-independent ones (see Supporting Information). Together with the data from the primary ALK inhibition assays (Table 3), these experiments suggest that the cytotoxicity of **32** is driven by the inhibitory activity against NPM-ALK phosphorylation.⁹

The pharmacokinetic parameters determined for **32** in Sprague–Dawley (S–D) rats and Scid mice are shown in Table 5. The compound was orally bioavailable and exhibited

Table 5. Pharmacokinetic Parameters of **32 in S–D Rats and in Scid Mice**

	PK parameters	S–D rat ^a	Scid mouse
iv	dose ^b (mg/kg)	1	1
	$t_{1/2}$ (h)	3.4 ± 0.2	6.0
	AUC _{0–t} (ng·h/mL)	1106 ± 74	7552
	V _d (L/kg)	3.5 ± 0.3	1.1
	CL (mL/min/kg)	12 ± 1.0	2
po	dose ^b (mg/kg)	5	10
	C _{max} (ng/mL)	392 ± 25	3473
	t_{max} (h)	6.0 ± 0.0	2.0
	$t_{1/2}$ (h)	nd	4.4
	AUC _{0–t} (ng·h/mL)	1765 ± 147	42534
	F%	43 ± 3	56

^aValues are means of data from three animals; standard deviations are indicated. ^bFormulated as solutions in: 3% DMSO, 30% Solutol, 67% PBS (i.v.); 100% PEG400 (p.o.).

high plasma exposures, long half-lives, and low clearance in both species. Oral bioavailability in mice was 56%, comparable to 43% in rat.

The results from the evaluation of **32** in single dose PK/PD experiments in Scid mice bearing subcutaneous ALK-dependent xenografts are shown in Figure 2. The pharmacodynamic effect achieved with a 30 mg/kg oral dose in Sup-M2 xenograft was 80–90% inhibition of NPM-ALK autophosphorylation over 12 h postdose (Figure 2A). The levels of compound in plasma reached 6–8 μ M for up to 12 h with a \sim 7-fold drop by the 24 h time point (Figure 2B). The levels in tumors were approximately 2-fold higher than in plasma at 12 h. These data suggested that twice a day dosing in efficacy studies would be appropriate.

The robust PD response observed in the single dose PK/PD experiments correlated well with the inhibition of tumor growth observed in the efficacy studies. In Sup-M2 xenografts (Figure 3) oral dosing for 12 days at 30 mg/kg bid effected partial tumor regression. Increasing the dose to 55 mg/kg bid resulted in complete tumor regression following 12 days of dosing. Importantly, no body weight loss or other overt toxicity was noticed with either of these dosing regimens.

CONCLUSIONS

In summary, we have described several chemical strategies to ameliorate bioactivation of lead structures in the 2-anilino-7-aryl-pyrrolo[2,1-*f*][1,2,4]triazine class of ALK inhibitors. Fluorination of the aniline ring substantially reduced metabolic bioactivation of piperazine derivatives, although complete mitigation was accompanied by loss of potency toward the target enzyme. Moving the piperazine to the *meta* position of the aniline ring also reduced bioactivation/conjugation; again, target potency suffered. Ultimately, replacing the piperazine-

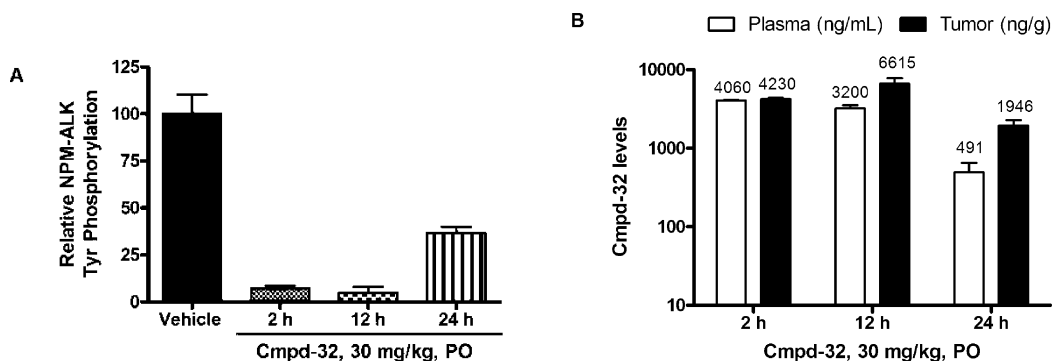


Figure 2. Results of PK/PD experiment in Sup-M2 xenograft in Scid mice: (A) inhibition of NPM-ALK autophosphorylation with a single dose of 32: 30 mg/kg po as a solution in PEG400; (B) compound concentration in plasma and tumor.

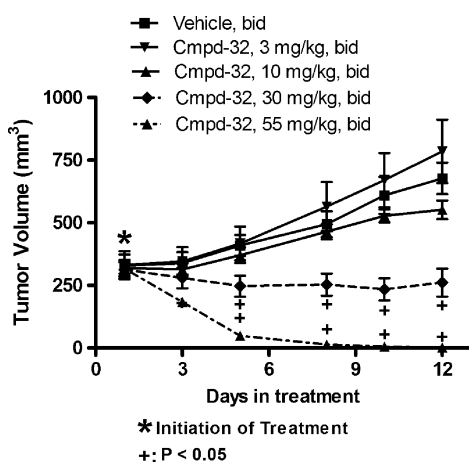


Figure 3. Antitumor efficacy of 32, dosed po as a solution in PEG400.

piperidine-containing pyrrolo[2,1-*f*][1,2,4]triazines proved successful. Interestingly, this replacement shifted metabolism to the core pyrrolotriazine for a subset of inhibitors containing a *N*-methyl(methylsulfonamide) moiety on the *C*7-aryl ring. We identified a product of oxidation at *C*5 and were able to block this position with a chlorine or methyl group to substantially improve in vitro stability while maintaining potency; these analogues displayed acceptable oral bioavailability. A *C*7 *o*-methoxyphenyl analogue (32) had excellent ALK activity, selectivity, and metabolic stability and displayed <1% in vitro bioactivation/conjugation. Furthermore, 32 was orally bioavailable in two species and demonstrated dose-related antitumor efficacy in ALK-driven tumor xenografts in mouse.

EXPERIMENTAL SECTION

General Methods. All commercial reagents and solvents were used as received unless otherwise indicated. ¹H and ¹³C NMR spectra were recorded on a Bruker Avance spectrometer at 400 and 100 MHz, respectively, in the solvent indicated, with tetramethylsilane as an internal standard. To assess the purity of the final compounds, analytical HPLC was run on a Zorbax RX-C8, 5 mm × 150 mm column, eluting with a 10–100% gradient mixture of acetonitrile and water containing 0.1% trifluoroacetic acid, over 5 min; purity, determined from the UV peak area, was ≥95%, unless indicated otherwise. UV detection was set at 254 and 290 nm wavelengths. LC/MS data were recorded on either of the following instruments: a Waters Acquity Ultra Performance LC coupled with Micromass LC-ZQ 2000 quadrupole mass spectrometer (2.1 mm × 50 mm Waters Acquity UPLC BEH C18 1.7 μm column, target column temperature 45 °C, run time 2 min, flow rate 0.600 mL/min, and solvent mixture of 5%

(0.1% formic acid/water):95% (acetonitrile/0.1% formic acid)), or a Bruker Esquire 200 ion trap. High resolution mass spectrometry was performed on a Waters Synapt G2 Q-TOF mass spectrometer by positive ion electrospray using leucine-enkephalin as a lock-mass standard. Automated column chromatography (SiO₂) was performed on CombiFlash Companion instruments (ISCO, Inc.). Melting points were taken on a Mel-Temp apparatus and are uncorrected.

4-(3-Methoxy-4-nitro-phenyl)-3,6-dihydro-2H-pyridine-1-carboxylic Acid *tert*-Butyl Ester (18). A mixture of 4-chloro-2-methoxy-1-nitro-benzene (4.9 g, 25.9 mmol), 4-(4,4,5,5-tetramethyl-1,3,2)dioxaborolan-2-yl)-3,6-dihydro-2H-pyridine-1-carboxylic acid *tert*-butyl ester (8.0 g, 25.9 mmol), tetrakis(triphenylphosphine)palladium(0) (1.5 g, 1.3 mmol), and a 2 M solution of potassium bicarbonate in water (32.5 mL, 65.0 mmol) in 1,4-dioxane (75 mL) was heated at 80 °C overnight. The reaction mixture was cooled to room temperature and partitioned between dichloromethane (200 mL) and water (200 mL). The layers were separated and the aqueous phase was extracted with dichloromethane (100 mL). The combined organic extracts were dried (MgSO₄) and then filtered, and the solvent was evaporated under reduced pressure. The product (8.5 g, 97% yield) was isolated by column chromatography (Silicagel, EtOAc/hexanes 25–50%). ¹H NMR (CDCl₃) δ 7.87 (d, *J* = 8.6 Hz, 1H), 7.01 (m, 2H), 6.17 (br s, 1H), 4.12 (m, 2H), 3.98 (s, 3H), 3.66 (m, 2H), 2.53 (m, 2H), 1.50 (s, 9H).

2-[4-(4-Amino-3-methoxy-phenyl)-piperidin-1-yl]-acetamide (19; R⁷ = CH₂C(O)NH₂). 4-(3-Methoxy-4-nitro-phenyl)-3,6-dihydro-2H-pyridine-1-carboxylic acid *tert*-butyl ester (3.0 g, 9.0 mmol) was treated with trifluoroacetic acid (3.5 mL, 44.9 mmol) in methylene chloride (20 mL) at room temperature for 2 h. Minimum amount of saturated sodium carbonate was added to pH 8, and the mixture was extracted with dichloromethane (3 × 100 mL). The combined extracts were dried (MgSO₄) and then filtered, and the solvent was evaporated under reduced pressure to afford 4-(3-methoxy-4-nitro-phenyl)-1,2,3,6-tetrahydro-pyridine (2.0 g, 95% yield), which was used in the next step without further purification. ¹H NMR (CDCl₃) δ 7.96 (d, *J* = 8.4 Hz, 1H), 7.02 (m, 2H), 6.28 (m, 1H), 3.98 (s, 3H), 3.598 (m, 2H), 3.13 (m, 2H), 2.46 (m, 2H), 1.76 (br s, 1H).

Into a 1-neck round-bottom flask was added 4-(3-methoxy-4-nitro-phenyl)-1,2,3,6-tetrahydro-pyridine (7.5 g, 32.0 mmol), iodoacetamide (5.9 g, 32.0 mmol), and cesium carbonate (15.7 g, 48.0 mmol) in acetonitrile (300 mL). The reaction was stirred overnight at reflux, and then cooled, when the product precipitated. Water was added and the product was collected by filtration, washed with water, and dried under high vacuum. Trituration from dichloromethane afforded the final product, 2-[4-(3-methoxy-4-nitro-phenyl)-3,6-dihydro-2H-pyridin-1-yl]-acetamide (7.4 g, 80% yield). ¹H NMR (CDCl₃) δ 7.87 (d, *J* = 8.3 Hz, 1H), 7.03 (m, 3H), 6.21 (m, 1H), 5.46 (br s, 1H), 3.99 (s, 3H), 3.31 (m, 2H), 3.17 (s, 2H), 2.85 (m, 2H), 2.60 (m, 2H).

To a solution of 2-[4-(3-methoxy-4-nitro-phenyl)-3,6-dihydro-2H-pyridin-1-yl]-acetamide (7.4 g, 25.5 mmol) in methanol (350 mL) was added 10% Pd/C (2.71 g). The mixture was shaken in a Parr apparatus under an atmosphere of hydrogen (50 PSI) for 2.5 h. Filtration

through Celite and evaporation of the solvent provided crude **19** (6.4 g, 95% yield), which was used without further purification. ^1H NMR (CDCl_3) δ 7.14 (br s, 1H), 6.65 (m, 3H), 5.39 (br s, 1H), 3.85 (s, 3H), 3.70 (br s, 2H), 3.03 (s, 2H), 2.98 (m, 2H), 2.42 (m, 1H), 2.28 (m, 2H), 1.85 (m, 2H), 1.73 (m, 2H).

General Procedure for the Synthesis of Inhibitors 12–15 and 22–40: 2-[4-(3-Methoxy-4-[7-(2-methoxy-phenyl)-pyrrolo[2,1-f][1,2,4]triazin-2-ylamino]-phenyl)-piperidin-1-yl]-acetamide (**32**). 7-(2-Methoxy-phenyl)-pyrrolo[2,1-f][1,2,4]triazin-2-ol (0.50 g, 2.1 mmol) was dissolved in *N,N*-dimethylformamide (40 mL) at 0 °C, and *N,N*-diisopropylethylamine (1.1 mL, 6.2 mmol) was added. The reaction stirred for 30 min, then *N*-phenylbis(trifluoromethanesulphonimide) (0.81 g, 2.3 mmol) was added and the reaction was allowed to warm to room temperature. After complete conversion to the corresponding trifluoromethanesulfonate intermediate (approximately 1 h; monitored by HPLC), 2-[4-(4-amino-3-methoxy-phenyl)-piperidin-1-yl]-acetamide (0.68 g, 2.6 mmol) was added and the reaction was heated at 95 °C overnight. *N,N*-Dimethylformamide was evaporated under reduced pressure, and the residue was partitioned between water (100 mL) and ethyl acetate (200 mL). The aqueous layer was further extracted with ethyl acetate (200 mL). The combined organic extracts were dried (MgSO_4), filtered, and the solvent evaporated under reduced pressure. The pure product (485 mg, 48% yield) was isolated by column chromatography (Silicagel, 0–10% MeOH/DCM), followed by Et_2O trituration to afford **32**. ^1H NMR (CDCl_3) δ 8.69 (s, 1H), 8.30 (d, J = 8.7 Hz, 1H), 8.00 (dd, J = 7.6, 1.5 Hz, 1H), 7.44 (m, 2H), 7.13 (m, 2H), 7.07 (d, J = 8.7 Hz, 1H), 7.03 (d, J = 4.6 Hz, 1H), 6.84 (d, J = 4.6 Hz, 1H), 6.72 (m, 2H), 5.42 (br s, 1H), 3.91 (s, 3H), 3.85 (s, 3H), 3.04 (s, 2H), 3.00 (m, 2H), 2.48 (m, 1H), 2.29 (m, 2H), 1.85 (m, 2H), 1.77 (m, 2H). ^{13}C NMR (CDCl_3) δ 173.7, 157.2, 152.5, 151.2, 147.5, 138.9, 131.1, 129.6, 127.9, 127.7, 121.1, 120.1, 119.4, 118.7, 117.8, 115.3, 111.0, 108.3, 105.1, 62.0, 55.7, 55.6, 54.9, 41.7, 33.9. LC/MS (ESI+) m/z 487.3 ($\text{M} + \text{H}$) $^+$; mp: 88–95 °C; high resolution mass spectrum (ESI) m/z 487.2457 [($\text{M} + \text{H}$) $^+$ calcd for $\text{C}_{27}\text{H}_{30}\text{N}_6\text{O}_3$; 487.2458].

***N*-[2-(2-{3-Fluoro-4-[4-(*S*)-2-hydroxy-propyl]-piperazin-1-yl]-2-methoxy-phenylamino)-pyrrolo[2,1-f][1,2,4]triazin-7-yl]-phenyl]-*N*-methylmethanesulfonamide, Trifluoroacetic Acid Salt (**11**).** ^1H NMR ($\text{DMSO}-d_6$) δ 9.48 (br s, 1H), 8.97 (s, 1H), 8.14 (s, 1H), 7.96 (m, 1H), 7.62 (m, 2H), 7.53 (m, 2H), 6.99 (dd, J = 15.0; 5.0 Hz, 2H), 6.70 (t, J = 8.0 Hz, 1H), 4.12 (m, 1H), 3.83 (m, 3H), 3.76 (m, 2H), 3.58 (m, 2H), 3.20 (m, 4H), 3.07 (s, 3H), 3.09 (s, 2H), 2.88 (s, 3H), 1.14 (d, J = 6.0 Hz, 3H). LC/MS (ESI+) m/z 584.0 ($\text{M} + \text{H}$) $^+$; HPLC purity 92%.

***N*-[2-(2-{5-Fluoro-4-[4-(*S*)-2-hydroxy-propyl]-piperazin-1-yl]-2-methoxy-phenylamino)-pyrrolo[2,1-f][1,2,4]triazin-7-yl]-phenyl]-*N*-methylmethanesulfonamide (**12**).** ^1H NMR ($\text{DMSO}-d_6$) δ 8.96 (s, 1H), 7.98 (d, J = 8.0 Hz, 1H), 7.84 (d, J = 15.0 Hz, 1H), 7.66 (m, 2H), 7.54 (m, 2H), 7.00 (dd, J = 17.0; 5.0 Hz, 2H), 6.68 (d, J = 8.0 Hz, 1H), 4.30 (m, 1H), 3.85 (s, 3H), 3.79 (m, 1H), 3.07 (s, 3H), 2.99 (m, 4H), 2.90 (s, 3H), 2.57 (m, 4H), 2.27 (m, 2H), 1.07 (d, J = 6.0 Hz, 3H); LC/MS (ESI+) m/z 584 ($\text{M} + \text{H}$); mp 116–120 °C.

***N*-[2-(2-{2,5-Difluoro-4-[4-(*S*)-2-hydroxy-propyl]-piperazin-1-yl]-phenylamino)-pyrrolo[2,1-f][1,2,4]triazin-7-yl]-phenyl]-*N*-methyl-methanesulfonamide, Trifluoroacetic Acid Salt (**13**).** ^1H NMR ($\text{DMSO}-d_6$) δ 9.54 (br, 1H), 8.99 (s, 1H), 8.88 (s, 1H), 7.96 (d, J = 8.0 Hz, 1H), 7.76 (m, 1H), 7.64 (d, J = 8.0 Hz, 1H), 7.49 (m, 2H), 7.06 (m, 1H), 7.00 (dd, J = 15.0; 5.0 Hz, 2H), 4.12 (m, 1H), 3.58 (d, J = 12.0 Hz, 2H), 3.44 (t, J = 12.0 Hz, 2H), 3.22 (m, 4H), 3.09 (s, 6H), 2.89 (s, 3H), 1.15 (d, J = 6.0 Hz, 3H); LC/MS (ESI+) m/z 572 ($\text{M} + \text{H}$).

***N*-[2-(2-[2-Methoxy-5-(4-methyl-piperazin-1-yl)-phenylamino]-pyrrolo[2,1-f][1,2,4]triazin-7-yl]-phenyl)-*N*-methyl-methanesulfonamide (**14**).** ^1H NMR (CDCl_3) δ 8.75 (s, 1H), 7.28 (s, 1H), 7.71 (m, 1H), 7.50 (m, 4H), 6.88 (br s, 2H), 6.78 (d, J = 8.6 Hz, 1H), 6.45 (d, J = 8.8 Hz, 1H), 3.87 (s, 3H), 3.16 (s, 3H), 2.75 (br s, 4H), 2.52 (s, 3H), 2.40 (br s, 4H), 2.35 (s, 3H). LC/MS (ESI+) m/z 522.0 ($\text{M} + \text{H}$) $^+$.

2-Methoxy-5-(4-methyl-piperazin-1-yl)-phenyl]-[7-(2-methoxy-phenyl)-pyrrolo[2,1-f][1,2,4]triazin-2-yl]-amine (15**).** ^1H NMR (CDCl_3) δ 8.69 (s, 1H), 7.95 (br s, 1H), 7.84 (d, J = 7.4 Hz, 1H), 7.52 (s, 1H), 7.40 (m, 1H), 7.08 (m, 2H), 6.93 (d, J = 3.7 Hz,

1H), 6.83 (d, J = 3.7 Hz, 1H), 7.76 (d, J = 8.6 Hz, 1H), 6.42 (d, J = 8.6 Hz, 1H), 3.85 (s, 3H), 3.82 (s, 3H), 2.85 (br s, 4H), 2.41 (br s, 4H), 2.34 (s, 3H). LC/MS (ESI+) m/z 445.1 ($\text{M} + \text{H}$) $^+$.

***N*-[2-(2-{4-[1-(2-Hydroxy-ethyl)-piperidin-4-yl]-2-methoxy-henylamino}-pyrrolo[2,1-f][1,2,4]triazin-7-yl)-phenyl]-*N*-methyl-methanesulfonamide (**22**).** ^1H NMR (CDCl_3) δ 8.72 (s, 1H), 8.07 (d, J = 8.4 Hz, 1H), 7.95 (m, 1H), 7.53 (m, 3H), 7.45 (s, 1H), 7.03 (d, J = 4.8 Hz, 1H), 6.86 (d, J = 4.8 Hz, 1H), 6.73 (d, J = 1.6 Hz, 1H), 6.64 (dd, J = 8.4, 1.6 Hz, 1H), 3.90 (s, 3H), 3.65 (m, 2H), 3.12 (s, 3H), 3.05 (m, 2H), 2.67 (s, 3H), 2.59 (m, 2H), 2.47 (m, 1H), 2.19 (m, 3H), 1.78 (m, 4H). LC/MS (ESI+) m/z 551.1 ($\text{M} + \text{H}$) $^+$; mp 99–111 °C.

***N*-[2-(2-{4-[1-(*R*)-2-Hydroxy-propyl]-piperidin-4-yl]-2-methoxy-phenylamino}-pyrrolo[2,1-f][1,2,4]triazin-7-yl)-phenyl]-*N*-methyl-methanesulfonamide (**23**).** ^1H NMR (CDCl_3) δ 8.72 (s, 1H), 8.07 (d, J = 8.4 Hz, 1H), 7.95 (d, J = 3.9 Hz, 1H), 7.53 (br s, 3H), 7.45 (s, 1H), 7.02 (d, J = 4.0 Hz, 1H), 6.86 (d, J = 3.9 Hz, 1H), 6.72 (s, 1H), 6.64 (d, J = 8.3 Hz, 1H), 3.90 (s, 3H), 3.89 (m, 1H), 3.15 (m, 1H), 3.12 (s, 3H), 2.95 (m, 1H), 2.67 (s, 3H), 2.37 (m, 4H), 2.05 (m, 1H), 1.79 (m, 4H), 1.26 (br s, 1H), 1.16 (d, J = 7.0 Hz, 3H). LC/MS (ESI+) m/z 565.2 ($\text{M} + \text{H}$) $^+$; mp 91–103 °C; HPLC purity 90%.

***N*-[2-(2-{2-Methoxy-4-piperidin-4-yl-phenylamino}-pyrrolo[2,1-f][1,2,4]triazin-7-yl)-phenyl]-*N*-methyl-methanesulfonamide (**24**).** ^1H NMR (CDCl_3) δ 8.72 (s, 1H), 8.08 (d, J = 8.4 Hz, 1H), 7.95 (m, 1H), 7.53 (m, 3H), 7.45 (s, 1H), 7.03 (d, J = 4.7 Hz, 1H), 6.86 (d, J = 4.7 Hz, 1H), 6.74 (s, 1H), 6.65 (d, J = 8.0 Hz, 1H), 3.89 (s, 3H), 3.23 (m, 2H), 3.12 (s, 3H), 2.76 (m, 2H), 2.67 (s, 3H), 2.57 (m, 1H), 2.30 (br s, 1H), 1.84 (m, 2H), 1.70 (m, 2H). LC/MS (ESI+) m/z 507.0 ($\text{M} + \text{H}$) $^+$; HPLC purity 92%.

(*R*)-1-(4-{3-Methoxy-4-[7-(2-methoxy-phenyl)-pyrrolo[2,1-f][1,2,4]triazin-2-ylamino]-phenyl]-piperidin-1-yl)-propan-2-ol (25**).** ^1H NMR (CDCl_3) δ 8.69 (s, 1H), 8.29 (d, J = 8.1 Hz, 1H), 7.99 (d, J = 7.7 Hz, 1H), 7.43 (m, 2H), 7.14 (m, 1H), 7.07 (d, J = 8.4 Hz, 1H), 7.02 (d, J = 4.4 Hz, 1H), 6.83 (d, J = 4.4 Hz, 1H), 6.73 (s, 1H), 6.71 (d, J = 8.1 Hz, 1H), 3.90 (s, 3H), 3.89 (m, 1H), 3.84 (s, 3H), 3.15 (m, 1H), 2.94 (m, 1H), 2.35 (m, 4H), 2.06 (m, 1H), 1.79 (m, 4H), 1.30 (br s, 1H), 1.16 (d, J = 5.8 Hz, 3H). LC/MS (ESI+) m/z 488.2 ($\text{M} + \text{H}$) $^+$; mp 67–74 °C. HPLC purity 94%.

[2-Methoxy-4-(1-methyl-piperidin-4-yl)-phenyl]-[7-(2-methoxy-phenyl)-pyrrolo[2,1-f][1,2,4]triazin-2-yl]-amine (26**).** ^1H NMR (CDCl_3) δ 8.69 (s, 1H), 8.29 (d, J = 8.8 Hz, 1H), 7.98 (dd, J = 8.0; 1.7 Hz, 1H), 7.42 (m, 2H), 7.12 (m, 1H), 7.07 (d, J = 8.4 Hz, 1H), 7.01 (d, J = 5.6 Hz, 1H), 6.83 (d, J = 5.6 Hz, 1H), 6.74 (s, 1H), 6.73 (m, 1H), 3.88 (s, 3H), 3.84 (s, 3H), 3.07 (m, 2H), 2.45 (m, 1H), 2.41 (s, 3H), 2.15 (m, 2H), 1.87 (m, 4H). LC/MS (ESI+) m/z 444.22 ($\text{M} + \text{H}$) $^+$; mp 71–84 °C.

(±)-1-Fluoro-3-(4-{3-methoxy-4-[7-(2-methoxy-phenyl)-pyrrolo[2,1-f][1,2,4]triazin-2-ylamino]-phenyl]-piperidin-1-yl)-propan-2-ol (27**).** ^1H NMR (CDCl_3) δ 8.69 (s, 1H), 8.29 (d, J = 8.8 Hz, 1H), 8.00 (dd, J = 7.6 Hz; 1.5 Hz, 1H), 7.44 (m, 2H), 7.14 (m, 1H), 7.08 (d, J = 8.3 Hz, 1H), 7.02 (d, J = 4.6 Hz, 1H), 6.83 (d, J = 4.6 Hz, 1H), 6.73 (s, 1H), 6.72 (d, J = 7.6 Hz, 1H), 4.44 (m, 2H), 3.95 (m, 1H), 3.91 (s, 3H), 3.85 (s, 3H), 3.10 (m, 1H), 2.95 (m, 1H), 2.47 (m, 4H), 2.10 (m, 1H), 1.80 (m, 4H), 1.59 (br s, 1 OH, and water peak). LC/MS (ESI+) m/z 506.0 ($\text{M} + \text{H}$) $^+$; mp 73–79 °C; HPLC purity 94%.

(*S*)-3-(4-{3-Methoxy-4-[7-(2-methoxy-phenyl)-pyrrolo[2,1-f][1,2,4]triazin-2-ylamino]-phenyl]-piperidin-1-yl)-propane-1,2-diol (28**).** ^1H NMR (CDCl_3) δ 8.69 (s, 1H), 8.29 (d, J = 8.0 Hz, 1H), 8.99 (dd, J = 8.0, 1.6 Hz, 1H), 7.44 (m, 2H), 7.13 (m, 1H), 7.07 (d, J = 8.0 Hz, 1H), 7.02 (d, J = 4.7 Hz, 1H), 6.83 (d, J = 4.7 Hz, 1H), 6.72 (s, 1H), 6.71 (d, J = 8.0 Hz, 1H), 3.90 (s, 3H), 3.86 (m, 1H), 3.85 (s, 3H), 3.77 (m, 1H), 3.55 (m, 1H), 3.22 (d, J = 10.6 Hz, 1H), 3.08 (d, J = 10.6 Hz, 1H), 2.77 (br s, 2H), 2.69 (m, 1H), 2.48 (m, 3H), 2.20 (m, 1H), 1.85 (m, 4H). LC/MS (ESI+) m/z 504.19 ($\text{M} + \text{H}$) $^+$; mp 66–80 °C.

2-Amino-1-(4-{3-methoxy-4-[7-(2-methoxy-phenyl)-pyrrolo[2,1-f][1,2,4]triazin-2-ylamino]-phenyl]-piperidin-1-yl)-2-methyl-propan-1-one (29**).** ^1H NMR (CDCl_3) δ 8.69 (s, 1H), 8.30 (d, J = 8.8 Hz, 1H), 7.99 (dd, J = 7.6; 1.6 Hz, 1H), 7.44 (m, 2H), 7.13 (m, 1H), 7.08 (d, J = 8.4 Hz, 1H), 7.02 (d, J = 4.7 Hz, 1H), 6.83 (d, J = 4.7 Hz, 1H), 6.70 (m, 2H), 4.84 (m, 2H), 3.89 (s, 3H), 3.84 (s, 3H), 2.88

(m, 2H), 2.72 (m, 1H), 1.90 (m, 2H), 1.63 (m, 4H), 1.45 (s, 6H). LC/MS (ESI+) m/z 515.0 (M + H)⁺; mp 81–89 °C.

(±)-Azetidin-2-yl-(4-{3-methoxy-4-[7-(2-methoxy-phenyl)-pyrrolo[2,1-f][1,2,4]triazin-2-ylamino]-phenyl}-piperidin-1-yl)-methanone (30). ¹H NMR (CDCl₃) δ 8.69 (s, 1H), 8.30 (m, 1H), 7.98 (m, 1H), 7.44 (m, 2H), 7.13 (m, 1H), 7.07 (d, *J* = 8.3 Hz, 1H), 7.03 (m, 1H), 6.84 (d, *J* = 4.6 Hz, 1H), 6.67 (m, 2H), 4.80 (m, 1H), 4.39 (m, 1H), 3.90 (s, 3H), 3.89* (s, 3H, *amide rotamer), 3.84 (s, 3H), 3.68 (m, 1H), 3.56 (m, 1H), 3.45 (m, 1H), 3.07 (m, 1H), 2.88 (m, 1H), 2.70 (m, 2H), 2.32 (m, 2H), 1.91 (m, 2H), 1.63 (m, 2H). LC/MS (ESI+) m/z 513.0 (M + H)⁺; mp 103–112 °C.

2-(4-{3-Methoxy-4-[7-(2-methoxy-phenyl)-pyrrolo[2,1-f][1,2,4]triazin-2-ylamino]-phenyl}-piperidin-1-yl)-N-methylacetamide (31). ¹H NMR (CDCl₃) δ 8.69 (s, 1H), 8.30 (d, *J* = 8.7 Hz, 1H), 8.00 (d, *J* = 6.3 Hz, 1H), 7.45 (m, 2H), 7.24 (m, 1H), 7.14 (m, 1H), 7.05 (d, *J* = 13.0 Hz, 1H), 7.03 (m, 1H), 6.84 (d, *J* = 4.7 Hz, 1H), 6.73 (m, 2H), 3.91 (s, 3H), 3.85 (s, 3H), 3.04 (s, 2H), 2.96 (m, 2H), 2.87 (d, *J* = 5.0 Hz, 3H), 2.47 (m, 1H), 2.29 (m, 2H), 1.73 (m, 4H). LC/MS (ESI+) m/z 501.21 (M + H)⁺; HPLC purity 91%.

2-(4-{4-[7-(2,4-Dimethoxy-phenyl)-pyrrolo[2,1-f][1,2,4]-[1,2,4]triazin-2-ylamino]-3-methoxy-phenyl}-piperidin-1-yl)-acetamide (33). ¹H NMR (MeOH-*d*₄) δ 8.78 (br s, 1H), 8.22 (d, *J* = 4.83 Hz, 1H), 7.77 (d, *J* = 4.87 Hz, 1H), 6.98 (s, 2H), 6.89 (s, 1H), 6.64–6.78 (m, 3H), 3.97 (s, 2H), 3.91 (s, 3H), 3.87 (s, 3H), 3.78 (s, 3H), 3.66–3.74 (m, 2H), 3.15–3.28 (m, 2H), 2.87 (m, 1H), 2.03–2.15 (m, 4H). LC/MS (ESI+) m/z 517.0 (M + H)⁺; mp 119–121 °C; HPLC purity 93%.

2-(4-{4-[7-(2-Cyano-phenyl)-pyrrolo[2,1-f][1,2,4]triazin-2-ylamino]-3-methoxy-phenyl}-piperidin-1-yl)-acetamide, Trifluoroacetic Acid Salt (34). ¹H NMR (DMSO-*d*₆) δ 9.51 (b s, 1H), 9.08 (s, 1H), 8.09 (d, *J* = 7.80 Hz, 1H), 8.05 (d, *J* = 7.80 Hz, 1H), 7.98 (s, 1H), 7.94 (d, *J* = 8.09 Hz, 1H), 7.88 (m, 2H), 7.72 (s, 1H), 7.65 (m, 1H), 7.17 (m, 1H), 7.04 (m, 1H), 6.90 (s, 1H), 6.71 (d, *J* = 8.20 Hz, 1H), 3.93 (s, 2H), 3.88 (s, 3H), 3.55 (d, *J* = 11.64 Hz, 2H), 3.15 (m, 2H), 2.67 (m, 1H), 2.01 (m, 4H). LC/MS (ESI+) m/z 482.17 (M + H)⁺.

2-(4-{3-Methoxy-4-[7-(3-methoxy-pyridin-2-yl)-pyrrolo[2,1-f][1,2,4]triazin-2-ylamino]-phenyl}-piperidin-1-yl)-acetamide, trifluoroacetic acid salt (35). ¹H NMR (DMSO-*d*₆) δ 9.48 (br s, 1H), 9.02 (s, 1H), 8.37 (d, *J* = 4.4 Hz, 1H), 8.14 (d, *J* = 8.2 Hz, 1H), 7.97 (s, 1H), 7.71 (m, 3H), 7.54 (dd, *J* = 8.4; 4.6 Hz, 1H), 7.07 (d, *J* = 4.6 Hz, 1H), 6.98 (d, *J* = 4.6 Hz, 1H), 6.88 (s, 1H), 6.71 (d, *J* = 8.4 Hz, 1H), 3.93 (s, 2H), 3.88 (s, 3H), 3.83 (s, 3H), 3.55 (m, 2H), 3.15 (m, 2H), 2.75 (m, 1H), 1.99 (m, 4H). LC/MS (ESI+) m/z 488.0 (M + H)⁺; HPLC purity 90%.

2-(4-{3-Methoxy-4-[7-(3-methoxy-pyridin-4-yl)-pyrrolo[2,1-f][1,2,4]triazin-2-ylamino]-phenyl}-piperidin-1-yl)-acetamide (36). ¹H NMR (CDCl₃) δ 8.75 (s, 1H), 8.48 (s, 1H), 8.43 (d, *J* = 4.0 Hz, 1H), 8.27 (d, *J* = 8.2 Hz, 1H), 8.21 (d, *J* = 4.0 Hz, 1H), 7.49 (s, 1H), 7.20 (d, *J* = 4.0 Hz, 1H), 7.19 (br s, 1H), 6.84 (d, *J* = 3.8 Hz, 1H), 6.79 (d, *J* = 8.3 Hz, 1H), 6.76 (s, 1H), 5.56 (br s, 1H), 3.99 (s, 3H), 3.92 (s, 3H), 3.05 (s, 2H), 3.02 (m, 2H), 2.49 (m, 1H), 2.31 (m, 2H), 1.79 (m, 4H). LC/MS (ESI+) m/z 488.0 (M + H)⁺; HPLC purity 92%.

2-(4-{4-[7-[2-(Methanesulfonyl-methyl-amino)-phenyl]-pyrrolo[2,1-f][1,2,4]triazin-2-ylamino]-3-methoxy-phenyl}-piperidin-1-yl)-acetamide (37). ¹H NMR (CDCl₃) δ 8.73 (s, 1H), 8.08 (d, *J* = 8.3 Hz, 1H), 7.95 (m, 1H), 7.53 (m, 3H), 7.46 (s, 1H), 7.12 (br s, 1H), 7.02 (d, *J* = 4.7 Hz, 1H), 6.86 (d, *J* = 4.7 Hz, 1H), 6.72 (d, *J* = 1.3 Hz, 1H), 6.64 (dd, *J* = 8.3, 1.3 Hz, 1H), 5.53 (br s, 1H), 3.90 (s, 3H), 3.13 (s, 3H), 3.04 (s, 2H), 2.99 (m, 2H), 2.66 (s, 3H), 2.46 (m, 1H), 2.29 (m, 2H), 1.85 (m, 2H), 1.75 (m, 2H). LC/MS (ESI+) m/z 564.17 (M + H)⁺; mp 103–112 °C; HPLC purity 94%.

2-(4-{4-[5-Hydroxy-7-[2-(methanesulfonyl-methyl-amino)-phenyl]-pyrrolo[2,1-f][1,2,4]triazin-2-ylamino]-3-methoxy-phenyl}-piperidin-1-yl)-acetamide (38). ¹H NMR (DMSO-*d*₆) δ 9.94 (s, 1H), 8.74 (s, 1H), 7.94–8.02 (m, 1H), 7.88 (d, *J* = 8.3 Hz, 1H), 7.59–7.67 (m, 1H), 7.48–7.56 (m, 2H), 7.40 (s, 1H), 7.21 (br s, 1H), 7.13 (br s, 1H), 6.85 (s, 1H), 6.67 (d, *J* = 8.3 Hz, 1H), 6.35 (s, 1H), 3.83 (s, 3H), 3.05 (s, 3H), 2.77–2.99 (m, 7H), 2.32–2.45

(m, 1H), 2.06–2.23 (m, 2H), 1.60–1.87 (m, 4H). LC/MS (ESI+) m/z 580.15 (M + H)⁺.

2-(4-{4-[7-[2-(Methanesulfonyl-methyl-amino)-phenyl]-5-methylpyrrolo[2,1-f][1,2,4]triazin-2-ylamino]-3-methoxy-phenyl}-piperidin-1-yl)-acetamide (39). ¹H NMR (DMSO-*d*₆) δ 8.95 (s, 1H), 7.93–7.98 (m, 1H), 7.88 (d, *J* = 8.2 Hz, 1H), 7.61–7.67 (m, 1H), 7.57 (s, 1H), 7.51–7.56 (m, 2H), 7.21 (s, 1H), 7.14 (s, 1H), 6.89 (s, 1H), 6.81 (s, 1H), 6.68 (d, *J* = 8.5 Hz, 1H), 3.84 (s, 3H), 3.05 (s, 3H), 2.85–2.95 (m, 7H), 2.35–2.45 (m, 4H), 2.08–2.28 (m, 2H), 1.64–1.81 (m, 4H). LC/MS (ESI+) m/z 578.16 (M + H)⁺.

2-(4-{4-[5-Chloro-7-[2-(methanesulfonyl-methyl-amino)-phenyl]-pyrrolo[2,1-f][1,2,4]triazin-2-ylamino]-3-methoxy-phenyl}-piperidin-1-yl)-acetamide (40). ¹H NMR (DMSO-*d*₆) δ 9.48 (br s, 1H), 8.98 (s, 1H), 7.95 (m, 3H), 7.79 (d, *J* = 8.1 Hz, 1H), 7.72 (s, 1H), 7.67 (d, *J* = 7.2 Hz, 1H), 7.55 (m, 2H), 7.01 (s, 1H), 6.88 (s, 1H), 6.68 (d, *J* = 8.2 Hz, 1H), 3.92 (s, 2H), 3.84 (s, 3H), 3.55 (m, 2H), 3.15 (m, 2H), 3.09 (s, 3H), 2.91 (s, 3H), 2.76 (m, 1H), 1.99 (m, 4H). LC/MS (ESI+) m/z 598.0 (M + H)⁺; HPLC purity 90%.

In Vitro Assays. ALK enzyme inhibition assay, cell-based NPM-ALK tyrosine phosphorylation assay, cytotoxicity assay, and caspase 3/7 activation assay were performed as described in ref 9. Metabolic stability assays in liver microsomes were performed as described in ref 17; metabolic stability assays in rat S9 fraction were performed in a similar manner. In vitro microsome incubations/GSH-trapping experiments were performed as described in ref 13.

In Vivo Assays. Rat and mouse pharmacokinetic assays, in vivo biochemical efficacy (PK/PD) assays, and antitumor efficacy studies were performed as described in refs 11a and 12.

■ ASSOCIATED CONTENT

Supporting Information

Additional biological data for compounds 25–30, 32, 39, and 40 and ¹H NMR and ¹³C NMR spectra for compound 32. This material is available free of charge via the Internet at <http://pubs.acs.org>.

■ AUTHOR INFORMATION

Corresponding Author

*Phone: 610-738-6168. Fax: 610-738-6643. E-mail: emesaros@cehalon.com.

■ ACKNOWLEDGMENTS

We thank Dr. Renee Roemmele and James Haley for assistance in multigram scale preparation of intermediates.

■ ABBREVIATIONS USED

ALK, anaplastic lymphoma kinase; ATP, adenosine triphosphate; AUC, area under the curve; bid, bis in die (twice a day); Cl, intrinsic clearance; C_{max} , maximum concentration; CYP, cytochrome P450; EML4, echinoderm microtubule-associated protein-like 4; *F*(%), fraction absorbed (oral bioavailability); GSH, glutathione; HPLC, high-pressure/performance liquid chromatography; IR, insulin receptor; iv, intravenous; LC, liquid chromatography; MS, mass spectrometry; NMR, nuclear magnetic resonance; NPM, nucleophosmin; PEG400, polyethyleneglycol-400; PK/PD, pharmacokinetic/pharmacodynamic; po, per os (oral); S(90), selectivity score 90% inhibition; SAR, structure–activity relationship; $t_{1/2}$, half-life; t_{max} , time of maximum concentration; TPM3, tropomyosin α -3 chain; V_d , volume of distribution

■ REFERENCES

(1) Manning, G.; Whyte, D. B.; Martinez, R.; Hunter, T.; Sundarsanam, S. The Protein Kinase Complement of the Human Genome. *Science* 2002, 298, 1912–1916.

- (2) (a) Chiarle, R.; Voena, C.; Ambrogio, C.; Piva, R.; Inghirami, G. The Anaplastic Lymphoma Kinase in the Pathogenesis of Cancer. *Nature Rev. Cancer* **2008**, *8*, 11–23. (b) Cheng, M.; Ott, G. R. Anaplastic Lymphoma Kinase as a Therapeutic Target in Anaplastic Large Cell Lymphoma, Non-Small Cell Lung Cancer and Neuroblastoma. *Anti-Cancer Agents Med. Chem.* **2010**, *10*, 236–249.
- (3) (a) Morris, S. W.; Kirstein, M. N.; Valentine, M. B.; Dittmer, K. G.; Shapiro, D. N.; Saltman, D. L.; Look, A. T. Fusion of a Kinase Gene, ALK, to a Nucleolar Protein Gene, NPM, in Non-Hodgkin's Lymphoma. *Science* **1994**, *263*, 1281–1284. (b) Palmer, R. H.; Vernersson, E.; Grabbe, C.; Hallberg, B. Anaplastic Lymphoma Kinase: Signalling in Development and Disease. *Biochem. J.* **2009**, *420*, 345–361.
- (4) (a) Soda, M.; Choi, Y. L.; Enomoto, M.; Takada, S.; Yamashita, Y.; Ishikawa, S.; Fujiwara, S.-i.; Watanabe, H.; Kurashina, K.; Hatanaka, H.; Bando, M.; Ohno, S.; Ishikawa, Y.; Aburatani, H.; Niki, T.; Sohara, Y.; Sugiyama, Y.; Mano, H. Identification of the Transforming EML4-ALK Fusion Gene in Non-Small-Cell Lung Cancer. *Nature* **2007**, *448*, 561–566. (b) Koivunen, J. P.; Mermel, C.; Zejnullahu, K.; Murphy, C.; Lifshits, E.; Holmes, A. J.; Choi, H. G.; Kim, J.; Chiang, D.; Thomas, R.; Lee, J.; Richards, W. G.; Sugarbaker, D. J.; DUCKO, C.; Lindeman, N.; Marcoux, J. P.; Engelman, J. A.; Gray, N. S.; Lee, C.; Meyerson, M.; Jaenke, P. A. EML4-ALK Fusion Gene and Efficacy of an ALK Kinase Inhibitor in Lung Cancer. *Clin. Cancer Res.* **2008**, *14*, 4275–4283.
- (5) Elenitoba-Johnson, K. S. J.; Crockett, D. K.; Schumacher, J. A.; Jenson, S. D.; Coffin, C. M.; Rockwood, A. L.; Lim, M. S. Proteomic Identification of Oncogenic Chromosomal Translocation Partners Encoding Chimeric Anaplastic Lymphoma Kinase Fusion Proteins. *Proc. Natl. Acad. Sci. U.S.A.* **2006**, *103*, 7402–7407.
- (6) (a) Lu, K. V.; Jong, K. A.; Kim, G. Y.; Singh, J.; Dia, E. Q.; Yoshimoto, K.; Wang, M. Y.; Cloughesy, T. F.; Nelson, S. F.; Mischel, P. S. Differential Induction of Glioblastoma Migration and Growth by Two Forms of Pleiotrophin. *J. Biol. Chem.* **2005**, *280*, 26953–26964. (b) George, R. E.; Sanda, T.; Hanna, M.; Froehling, S.; Luther, W. II; Zhang, J.; Ahn, Y.; Zhou, W.; London, W. B.; McGrady, P.; Xue, L.; Zozulya, S.; Gregor, V. E.; Webb, T. R.; Gray, N. S.; Gilliland, D. G.; Diller, L.; Greulich, H.; Morris, S. W.; Meyerson, M.; Look, A. Activating Mutations in ALK Provide a Therapeutic Target in Neuroblastoma. *Nature* **2008**, *455*, 975–978.
- (7) (a) Milkiewicz, K. L.; Ott, G. R. Inhibitors of Anaplastic Lymphoma Kinase: a Patent Review. *Expert Opin. Ther. Pat.* **2010**, *20*, 1653–1681. (b) Webb, T. R.; Slavish, J.; George, R. E.; Look, A. T.; Xue, L.; Jiang, Q.; Cui, X.; Rentrop, W. B.; Morris, S. W. Anaplastic Lymphoma Kinase: Role in Cancer Pathogenesis and Small-Molecule Inhibitor Development for Therapy. *Expert Rev. Anticancer Ther.* **2009**, *9*, 331–356.
- (8) (a) Christensen, J. G.; Zou, H. Y.; Arango, M. E.; Li, Q.; Lee, J. H.; McDonnell, S. R.; Yamazaki, S.; Alton, G. R.; Mroczkowski, B.; Los, G. Cytoreductive Antitumor Activity of PF-2341066, a Novel Inhibitor of Anaplastic Lymphoma Kinase and c-Met, in Experimental Models of Anaplastic Large-Cell Lymphoma. *Mol. Cancer Ther.* **2007**, *6*, 3314–3322. (b) Zou, H. Y.; Li, Q.; Lee, J. H.; Arango, M. E.; McDonnell, S. R.; Yamazaki, S.; Koudriakova, T. B.; Alton, G.; Cui, J. J.; Kung, P.-P.; Nambu, M. D.; Los, G.; Bender, S. L.; Mroczkowski, B.; Christensen, J. G. An Orally Available Small-Molecule Inhibitor of c-Met, PF-2341066, Exhibits Cytoreductive Antitumor Efficacy through Antiproliferative and Antiangiogenic Mechanisms. *Cancer Res.* **2007**, *67*, 4408–4417. (c) *An Investigational Drug, PF-02341066 Is Being Studied Versus Standard of Care in Patients with Advanced Non-Small Cell Lung Cancer with a Specific Gene Profile Involving the Anaplastic Lymphoma Kinase (ALK) Gene*; National Institutes of Health: Bethesda, MD, 2009; <http://www.clinicaltrials.gov/ct2/show/NCT00932893>. (d) PF-2341066 (Crizotinib) has recently received FDA approval for ALK-positive lung cancer. U.S. Food and Drug Administration, Center for Drug Evaluation and Research. Xalkori NDA 202570, approval letter, August 26, 2011. http://www.accessdata.fda.gov/drugsatfda_docs/appletter/2011/202570s000ltr.pdf. (e) Sakamoto, H.; Tsukaguchi, T.; Hiroshima, S.; Kodama, T.; Kobayashi, T.; Fukami, T. A.; Oikawa, N.; Tsukuda, T.; Ishii, N.; Aoki, Y. CH5424802, a Selective ALK Inhibitor Capable of Blocking the Resistant Gatekeeper Mutant. *Cancer Cell* **2011**, *19*, 679–690.
- (9) Wan, W.; Albom, M. S.; Lu, L.; Quail, M. R.; Becknell, N. C.; Weinberg, L. R.; Reddy, D. R.; Holskin, B. P.; Angeles, T. S.; Underiner, T. L.; Meyer, S. L.; Hudkins, R. L.; Dorsey, B. D.; Ator, M. A.; Ruggeri, B. A.; Cheng, M. Anaplastic Lymphoma Kinase Activity is Essential for the Proliferation and Survival of Anaplastic Large-Cell Lymphoma Cells. *Blood* **2006**, *107*, 1617–1623.
- (10) Milkiewicz, K. L.; Weinberg, L. R.; Albom, M. S.; Angeles, T. S.; Cheng, M.; Ghose, A. K.; Roemmele, R. C.; Theroff, J. P.; Underiner, T. L.; Zificsak, C. A.; Dorsey, B. D. Synthesis and Structure–Activity Relationships of 1,2,3,4-Tetrahydropyrido[2,3-*b*]pyrazines as Potent and Selective Inhibitors of the Anaplastic Lymphoma Kinase. *Bioorg. Med. Chem.* **2010**, *18*, 4351–4362.
- (11) (a) Ott, G. R.; Tripathy, R.; Cheng, M.; McHugh, R.; Anzalone, A. V.; Underiner, T. L.; Curry, M. A.; Quail, M. R.; Lu, L.; Wan, W.; Angeles, T. S.; Albom, M. S.; Aimone, L. D.; Ator, M. A.; Ruggeri, B. A.; Dorsey, B. D. Discovery of a Potent Inhibitor of Anaplastic Lymphoma Kinase with in Vivo Antitumor Activity. *ACS Med. Chem. Lett.* **2010**, *1*, 493–498. (b) Mesaros, E. F.; Burke, J. P.; Parrish, J. D.; Dugan, B. J.; Anzalone, A. V.; Angeles, T. S.; Albom, M. S.; Aimone, L. D.; Quail, M. R.; Wan, W.; Lu, L.; Huang, Z.; Ator, M. A.; Ruggeri, B. A.; Cheng, M.; Ott, G. R.; Dorsey, B. D. Novel 2,3,4,5-Tetrahydrobenzo[*d*]azepine Derivatives of 2,4-Diaminopyrimidine, Selective and Orally Bioavailable ALK Inhibitors with Antitumor Efficacy in ALCL Mouse Models. *Bioorg. Med. Chem. Lett.* **2011**, *21*, 463–466. (c) Zificsak, C. A.; Theroff, J. P.; Aimone, L. D.; Albom, M. S.; Angeles, T. S.; Cheng, M.; Mesaros, E. F.; Ott, G. R.; Quail, M. R.; Underiner, T. L.; Wan, W.; Dorsey, B. D. Methanesulfonamido-cyclohexylamine Derivatives of 2,4-Diaminopyrimidine as Potent ALK Inhibitors. *Bioorg. Med. Chem. Lett.* **2011**, *21*, 3877–3880.
- (12) Ott, G. R.; Wells, G. J.; Thieu, T. V.; Quail, M. R.; Lisko, J. G.; Mesaros, E. F.; Gingrich, D. E.; Ghose, A. K.; Wan, W.; Lu, L.; Cheng, M.; Albom, M. S.; Angeles, T. S.; Huang, Z.; Aimone, L. D.; Ator, M. A.; Ruggeri, B. A.; Dorsey, B. D. 2,7-Disubstituted-pyrrolo[2,1-*f*][1,2,4]triazines: new variant of an old template and application to the discovery of anaplastic lymphoma kinase (ALK) inhibitors with in vivo antitumor activity. *J. Med. Chem.* **2011**, *54*, 6328–6341.
- (13) A detailed account, including experimental protocols, has been reported elsewhere. Wells-Knecht K. J.; Ott, G. R.; Cheng, M.; Wells, G. J.; Breslin, H. J.; Gingrich, D. E.; Weinberg, L. R.; Mesaros, E. F.; Huang, Z.; Yazdani, M.; Ator, M. A.; Aimone, L. D.; Zeigler, K.; Dorsey, B. D. 2,7-Disubstituted-pyrrolo[2,1-*f*]triazine kinase inhibitors with an unusually high degree of reactive metabolite formation. *Chem. Res. Toxicol.* **2011**, *24*, 1994–2003.
- (14) For a recent review on reactive metabolites in drug discovery see: Park, B. K.; Boobis, A.; Clarke, S.; Goldring, C. E. P.; Jones, D.; Kenna, J. G.; Lambert, C.; Laverty, H. G.; Naisbitt, D. J.; Nelson, S.; Nicoll-Griffith, D. A.; Obach, R. S.; Routledge, P.; Smith, D. A.; Tweedie, D. J.; Vermeulen, N.; Williams, D. P.; Wilson, I. D.; Baillie, T. A. Managing the Challenge of Chemically Reactive Metabolites in Drug Development. *Nature Rev. Drug Discovery* **2011**, *10*, 292–306.
- (15) Thieu, T.; Sclafani, J. A.; Levy, D. V.; McLean, A.; Breslin, H. J.; Ott, G. R.; Bakale, R.; Dorsey, B. D. Discovery and Process Synthesis of Novel 2,7-Pyrrolo[2,1-*f*][1,2,4]triazines. *Org. Lett.* **2011**, *13*, 4204–4207.
- (16) Walker, D. P.; Bi, C.; Kalgutkar, A. S.; Bauman, J. N.; Zhao, S. X.; Soglia, J. R.; Aspnes, G. E.; Kung, D. W.; Klug-McLeod, J.; Zawistowski, M. P.; McGlynn, M. A.; Oliver, R.; Dunn, M.; Li, J.-C.; Richter, D. T.; Cooper, B. A.; Kath, J. C.; Hulford, C. A.; Autry, C. L.; Luzzio, M. J.; Ung, E. J.; Roberts, W. G.; Bonnette, P. C.; Buckbinder, L.; Mistry, A.; Griffor, M. C.; Han, S.; Guzman-Perez, A. Trifluoromethylpyrimidine-Based Inhibitors of Proline-Rich Tyrosine Kinase 2 (PYK2): Structure–Activity Relationships and Strategies for the Elimination of Reactive Metabolite Formation. *Bioorg. Med. Chem. Lett.* **2008**, *18*, 6071–6077.
- (17) Weinberg, L. R.; Albom, M. S.; Angeles, T. S.; Breslin, H. J.; Gingrich, D. E.; Huang, Z.; Lisko, J. G.; Mason, J. L.; Milkiewicz, K. L.; Thieu, T. V.; Underiner, T. L.; Wells, G. J.; Wells-Knecht, K. J.

Dorsey, B. D. 2,7-Pyrrolo[2,1-f][1,2,4]triazines as JAK2 inhibitors: Modification of target structure to minimize reactive metabolite formation. *Bioorg. Med. Chem. Lett.* **2011**, *21*, 7325–7330.

(18) Sabbatini, P.; Korenchuk, S.; Rowand, J. L.; Groy, A.; Liu, Q.; Leperi, D.; Atkins, C.; Dumble, M.; Yang, J.; Anderson, K.; Kruger, R. G.; Gontarek, R. R.; Maksimchuk, K. R.; Suravajjala, S.; Lapierre, R. R.; Shotwell, J. B.; Wilson, J. W.; Chamberlain, S. D.; Rabindran, S. K.; Kumar, R. GSK1838705A Inhibits the Insulin-like Growth Factor-1 Receptor and Anaplastic Lymphoma Kinase and Shows Antitumor Activity in Experimental Models of Human Cancers. *Mol. Cancer Ther.* **2009**, *8*, 2811–2820.

(19) Karaman, M. W.; Herrgard, S.; Treiber, D. K.; Gallant, P.; Atteridge, C. E.; Campbell, B. T.; Chan, K. W.; Ciceri, P.; Davis, M. I.; Edeen, P. T.; Faraoni, R.; Floyd, M.; Hunt, J. P.; Lockhart, D. J.; Milanov, Z. V.; Morrison, M. J.; Pallares, G.; Patel, H. K.; Pritchard, S.; Wodicka, L. M.; Zarrinkar, P. P. A Quantitative Analysis of Kinase Inhibitor Selectivity. *Nature Biotechnol.* **2008**, *26*, 127–132.